Proceedings of the ASME 2014 Dynamic Systems and Control Conference
DSCC 2014
October 22-24, 2014, San Antonio, TX, USA

DSCC2014-6110

VISUAL FEEDBACK BASED DROPLET SIZE REGULATION IN ELECTROHYDRODYNAMIC JET PRINTING

Berk Altın *
Department of Electrical Engineering and Computer Science
University of Michigan, Ann Arbor
Ann Arbor, Michigan 48109
Email: altin@umich.edu

Leo Tse
Kira Barton
Department of Mechanical Engineering
University of Michigan, Ann Arbor
Ann Arbor, Michigan 48109
Email: tselaiyu@umich.edu, bartonkl@umich.edu

ABSTRACT

Electrohydrodynamic jet (e-jet) printing is a recent micromanufacturing technique that uses electrostatic force to draw out ink from a conductive nozzle onto a conductive substrate. While the advantages (high speed and resolution, flexibility) of e-jet printing over ink jet printing and other microfabrication methods are abundant, precise control of the process is necessary for successful commercialization of the technology. This paper shows how visual feedback through image processing may be used to regulate the volume of printed droplets for increased manufacturing precision.

INTRODUCTION

Graphic arts printing techniques for additive micromanufacturing have drawn considerable attention in recent years due to flexibility, high resolution, and low cost. Conventional ink jet printing methods use thermal or piezoelectric excitation to deposit ink material onto the substrate. The flexibility of ink jet printing technologies, as opposed to other microfabrication methods, stems from the abundance of compatible materials and the ability to easily accommodate new designs through software (as opposed to hardware) changes. Nevertheless, functional resolutions of these processes are limited to 20-30 μm, which restrict their usage in high precision applications in the submicron level [1].

A recent jet printing technique that uses electrostatic force to draw out ink from a conductive microcapillary nozzle onto the substrate is electrohydrodynamic jet (e-jet) printing. E-jet printing offers superior resolution compared to conventional ink jets, with resolutions well below 1 μm, and high printing speeds on the kHz range. Furthermore, e-jet printing has found diverse applications such as printed circuitry [2,3], hydrogel patterning [4], cell deposition on surfaces [5] and biosensors [6]. Despite these promising features, precision control of e-jet printing is necessary for successful commercialization of the technology [7]. In that regard, the two outputs to be controlled can be listed as droplet position and diameter. Assuming that the motion stages that move the substrate achieve perfect tracking with respect to a desired position signal, the droplet position is directly determined by the jetting frequency of the process. Initial works using a current detection based approach have proven beneficial for more consistent droplet spacing [7], with a reduction in errors up to 65%. However, the control scheme was limited to the direct current (DC) mode of printing, which provides limited controllability due to the implicit dependence between jetting frequency and droplet diameter. On the other hand, to the best of our knowledge, closed loop droplet size regulation in e-jet printing has never been tried before.

This paper demonstrates how visual feedback through image processing may be used to regulate droplet diameters for increased manufacturing precision in e-jet printing. We rely on the pulsed mode of operation, which gives additional flexibility in the process with the capability to control jetting frequency and droplet diameter independently [8]. We use a high resolution

*Address all correspondence to this author.

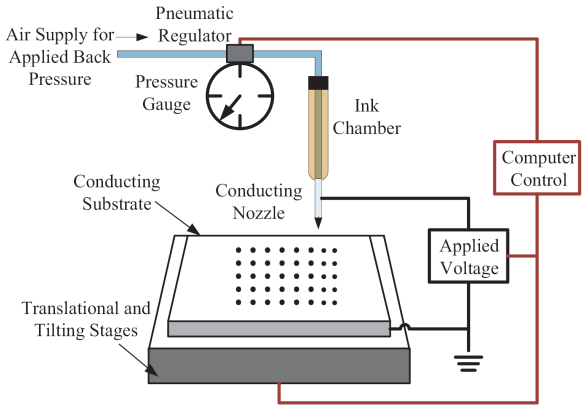

FIGURE 1. SCHEMATIC OF AN E-JET PRINTER WITH THE MAIN COMPONENTS [8].

camera focused on the tip of the conductive nozzle to monitor meniscus formation online, and employ image processing to extract the height of the ink meniscus. The extracted height signal is regulated by an empirically tuned feedback controller to improve precision. Note that although the actual output to be controlled is the droplet diameter, meniscus regulation provides additional controllability of the system by providing information about the system between successive droplets, thereby presenting the opportunity to reduce errors in droplet size by controlling the dynamics of meniscus formation. On the other hand, sensing of the printed droplets gives limited information about the process dynamics. Furthermore, assuming a discrete time linear system sampled at jetting frequency, any feedback controller acting on such a measurement scheme would suffer from a one step delay.

The rest of the paper is organized as follows. First, we provide a short review of e-jet printing and present fundamental components that make up the printer. We describe existing literature about e-jet printing dynamics. We present the implementation of the proposed image sensing scheme. We then give details about our experimental setup and discuss the results. Finally, we give concluding remarks.

E-JET PRINTING

The main components of an e-jet printer are illustrated in Fig. 1. The fundamental parameters of the process are the standoff (or offset) height h_s and the voltage V_h between the nozzle and the substrate, along with the pneumatic pressure. The ink material is kept at the tip of the nozzle by the back pressure supplied to the ink chamber, which ensures that a fluid meniscus can form readily by the application of a potential difference. A high enough voltage induces the deformation of the meniscus into a conical shape, called the Taylor cone, which jets a droplet onto the substrate when the electrostatic force overcomes the surface tension [8,9].

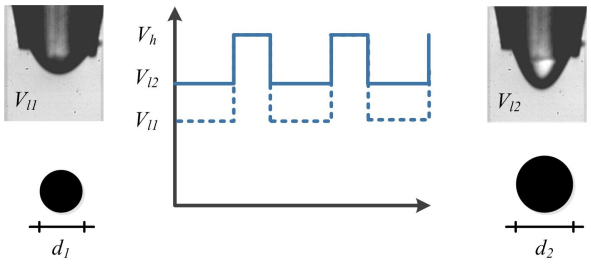

FIGURE 2. PULSED MODE OF OPERATION. THE MAGNITUDE OF THE BASELINE VOLTAGE DETERMINES THE DIAMETER OF PRINTED DROPLETS WHEN THE OTHER PROCESS PARAMETERS ARE FIXED.

PROCESS MODELING AND CONTROLLABILITY

Current e-jet printers run generally in an open loop setting. Apart from the difficulties in sensing, one of the main reasons for this approach is the lack of a proper dynamic model. Static nonlinear relationships that provide useful information about the process are identified in [9], given by

$$f \propto \left(\frac{\varepsilon_0^3}{d_n^3 \rho^2 \gamma}\right)^{1/4} E^{3/2}, \quad d \propto \left(\frac{d_n \gamma}{\varepsilon_0}\right)^{1/2} E^{-1}, \tag{1}$$

where f is the jetting frequency, ε_0 is the permittivity of free space, d_n is the nozzle diameter, ρ is the density of the ink material, γ is the surface tension of the air-ink interface, E is the magnitude of the electric field between the nozzle and the substrate, and d is the diameter of the jet. The electric field is approximated by the equality $E = 4V_h/(d_n \ln(8h_s/d_n))$, which when substituted to Eq. 1 yields

$$f \propto \alpha \left(\frac{V_h}{g(h_s)}\right)^{3/2}, \quad d \propto \beta \frac{g(h_s)}{V_h}, \tag{2}$$

where α and β are constants such that $\alpha \triangleq 8(\varepsilon_0^3/(d_n^9 \rho^2 \gamma))^{1/4}$ and $\beta \triangleq 0.25((d_n^3 \gamma)/\varepsilon_0)^{1/2}$, and g is a function of h_s so that $g(h_s) \triangleq \ln(8hs/d_n)$.

Although early efforts have shown the potential of current sensing based feedback and learning control of the jetting frequency as a means of regulating droplet spacing [7], it is obvious from Eq. 2 that given a certain ink material and nozzle, when the standoff height h_s is fixed, constant voltage operation provides a single degree of freedom, wherein either f or d can be controlled. Also observe that while a high potential difference implies a faster printing frequency, this results in increased sensitivity to process parameters, thereby leading to inconsistent droplet spacing.

PULSED MODE OF THE E-JET PROCESS

To overcome this limitation, a pulsed voltage mode of operation was suggested [8], where a lower baseline voltage V_l is employed to keep the meniscus at a desired height, and a higher voltage spike (V_h) is used to break the meniscus and deposit the material. Recall from Eq. 2 that an increased potential difference results in a faster printing frequency. When f is very fast compared to the motion stages, successive droplets merge on the substrate surface to form a single larger droplet. Thus, the total volume v^j of ink printed on the substrate during pulse j is

$$\sum_{k=1}^{\lfloor T_p f \rfloor} v_k, \tag{3}$$

where T_p is the pulse width, v_k is the volume of the k-th droplet during pulse j, and $\lfloor . \rfloor$ is the floor function. Also note that when the process is subject to random variations, the empirical variance of v^j is likely to decrease to as T_p is increased due to averaging.

The baseline voltage preserves the charge in the meniscus so that jetting dynamics are quickly excited and the droplets are released on demand during each pulse peak. In dynamic systems terms, V_l ensures fast convergence to steady state by ensuring that the initial condition at the beginning of the pulse is relatively close to the DC behavior of the process with voltage V_h. Hence, V_l should be chosen so that there is no jetting prior to the pulse, yet it must be high enough for fast operation. The frequency of the pulse can then be directly tuned to control spacing of these aggregate droplets, independent of the droplet size. Further details on the pulsed mode of e-jet printing can be found in [8].

IMAGE SENSING BASED FEEDBACK

Our approach relies on the pulsed mode of operation due to its drop on demand capability, which ensures high resolution printing with speeds that are several orders of magnitude faster than that of constant voltage operation. Observe in Fig. 2 that there is a positive correlation between the droplet size and the meniscus size prior to jetting. This implies that for a fixed pulse width, peak voltage and standoff height, the baseline voltage can be used to regulate the droplet size around a fixed set point, since increasing voltages (below the jetting voltage) signify a larger meniscus due to increasing electrostatic force. This phenomenon can explained by the terminology of the previous section as follows: If T_p is relatively high, v^j, the total volume of ink deposited during pulse j is less likely to be affected by V_l since a quasistatic analysis based on Eq. 2 would be valid. However, when T_p is low, v^j varies depending on V_l due to the dynamics of the jetting process.

To take advantage of this relationship, we use a stationary camera that is focused on the nozzle to estimate changes in meniscus height. The high resolution image obtained through the camera is first cropped to decrease computational load, then converted to binary (black and white) as shown in Fig. 3. The threshold for the conversion is determined adaptively using Otsu's method [10], which differentiates the background from the foreground (the nozzle) using a statistical approach: Assuming two different classes (background and object) in a grayscale image with N pixels, the objective is to maximize interclass variance calculated according to the probability mass function derived by normalizing the gray level histogram, so that the probability of selecting a pixel with intensity $i \in \{0, 1, \ldots, i_{max}\}$ is given by n_i/N, where n_i is the number of pixels with intensity i.

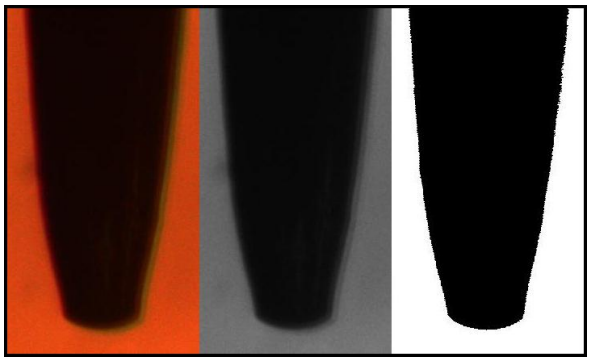

FIGURE 3. CONVERSION OF THE IMAGE TO GRAYSCALE AND BINARY. THE THRESHOLD IS DETERMINED VIA OTSU'S METHOD.

The height data h is extracted by finding the last row of the binary image with a false, or black, pixel. The error signal $e = r - h$, where r is the reference height, is then fed into a simple proportional-integral-derivative (PID) controller. Afterwards, the control input computed according to the PID control law is added to the nominal baseline voltage to regulate the meniscus prior to jetting. Note that the calculated height is not that of the meniscus, but the combined height of the meniscus with the nozzle. Hence, r must be set accordingly.

EXPERIMENTAL SETUP AND RESULTS

The desktop e-jet printer that we will use in verifying our approach is shown in Fig. 4. The main components of interest are the Aerotech X, Y, Z stages, Trek high voltage amplifier, Edmund Optics zoom lens and fiber optic illuminator, and Lumenera high resolution camera. The positioning stages, camera, and the voltage supply are all controlled through a LabVIEW graphical user interface. The stages have a resolution of 1 μm, while the camera has a resolution of 2 megapixels. The magnification power of the zoom lens is 10x. The fiber optic illuminator is adjusted to create a contrast between the nozzle and the background to facilitate image processing, as can be seen in Fig. 3. The measured resolution of the images is roughly 0.14 μm/pixel.

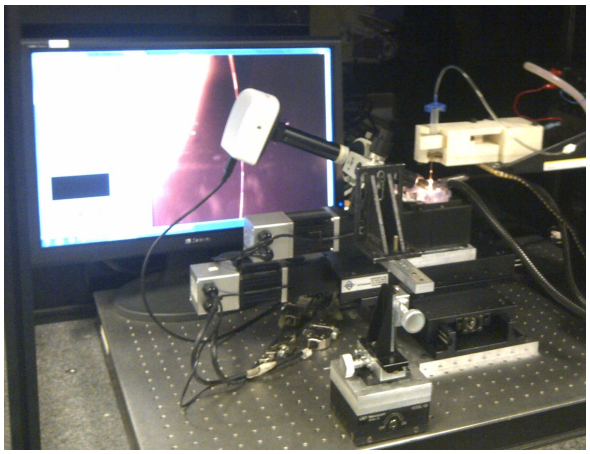

FIGURE 4. 4 AXIS EXPERIMENTAL TESTBED FOR E-JET PRINTING WITH HIGH RESOLUTION CAMERA.

To verify the validity of image sensing as a valid approach for feedback control, we will compare the trials listed below:

1. Open loop printing at 75 μm offset; 52 droplets.
2. Open loop printing at 85 μm offset; 52 droplets.
3. Closed loop printing at 75 μm offset; 52 droplets.
4. Closed loop printing at 85 μm offset; 52 droplets.

The objective of the trials is to show that closed loop operation maintains a more consistent average droplet size in the two offsets, compared to the open loop case. Here, assuming a one-to-one correspondence between the diameter and volume of printed droplets, we will take the average droplet diameter of a given trial as our performance metric. That is, given average droplet diameters of d_1, d_2, d_3, and d_4 for the four cases, we would like to see $|d_3 - d_4| < |d_1 - d_2|$.

The printing parameters for the experiment are shown in Table 1. The voltage parameters V_l and V_h are tuned for a 75 μm offset. So ideally, we would have $d_1 \approx d_3 \approx d_4$. However, because we have a 10 μm difference in the offset height, we expect to see $d_1 \approx d_3 > d_4 > d_2$, with $d_3 - d_4$ significantly smaller than $d_1 - d_2$. This is because even with perfect meniscus regulation, a larger offset implies a weaker electrostatic force and therefore less fluid flow. The pulse width T_p is chosen relatively high to ensure jetting in both cases for the same reason: Since the electrostatic force decreases with increasing offset, a lower value for T_p results in no printing for cases 2 and 4. To see how the standoff height affects the droplet diameters, assume for simplicity that the volume of each droplet from a single jet is equal and a linear function of the jet diameter d such that $v_k = \lambda d$ for some constant λ. Then, from Eq. 2 and 3

$$v^j \approx T_p f v_k = \alpha\beta\lambda T_p \left(\frac{V_h}{g(h_s)}\right)^{1/2}. \quad (4)$$

TABLE 1. PRINTING PARAMETERS.

Parameter	Value
Ink	NOA 81
Nozzle diameter	30 μm
Back Pressure	0 psi
Baseline Voltage (V_l)	520 V
Peak Voltage (V_h)	800 V
Pulse Width (T_p)	20 ms
Pulsing Frequency	0.2 Hz
Image Sampling Frequency	5 Hz
Proportional Gain (K_p)	10 V/pixel
Integral Gain (K_i)	0.5 V/pixel
Derivative Gain (K_d)	1 V/pixel

Thus, v^j decreases as h_s increases.

In implementing the PID controller on the system, we take h as the 3 point moving average of the output of the image processing algorithm to smooth out the noise due to mechanical vibrations of the setup. The algorithm samples the height signal at a rate of 5 Hz. This rate is chosen to decrease computational load and is limited by the 12 frames per second capacity of the camera. Because of the low sampling rate, lack of information about the process dynamics, and because a large enough increment to the baseline can result in unwanted jetting, the controller gains are adjusted cautiously to the values shown in Table 1 using standard manual PID tuning guidelines. To allow sufficient time for the meniscus to settle, the printing frequency is chosen as 0.2 Hz. For closed loop operation, we approximate r to be the measured meniscus height at 75 μm offset with a DC input of magnitude V_l.

Figure 5 presents selected printing results for the four different cases. Note that both the open loop and closed loop cases show similar droplet diameters with $d_1 \approx 43\mu$m and $d_3 \approx 40\mu$m. The difference between d_1 and d_3 can be attributed to measurement noise, or an erroneous r since we do not know the actual mapping between h and the droplet diameters. At 85 μm standoff, we see that while both open and closed loop shows higher variances, the closed loop performs significantly better than open loop with $d_2 \approx 27\,\mu$m and $d_4 \approx 30\,\mu$m. This corresponds to a‘37% decrease in droplet diameter in open loop and a 25% decrease in closed loop. While the closed loop error still seems high, this is expected due to the fact that the 10 μm increase in offset height provides a significant decrease in the electrostatic

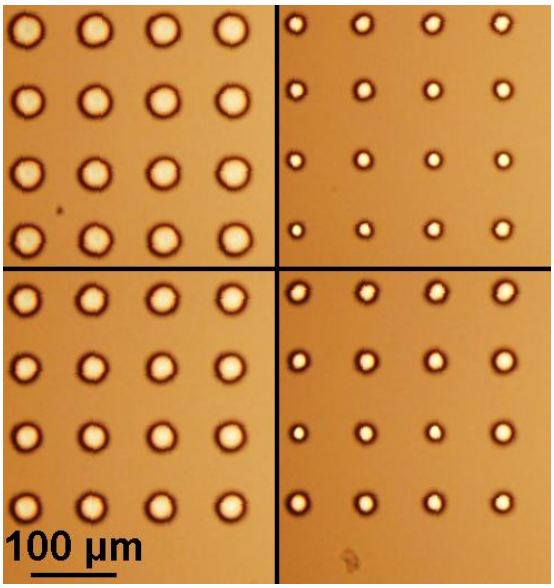

FIGURE 5. PRINTING RESULTS IN OPEN LOOP (TOP) AND CLOSED LOOP (BOTTOM), AT 75 (LEFT) AND 85 (RIGHT) MICROMETERS OFFSET.

force. Even with perfect meniscus regulation, a lower electrostatic force naturally draws out less material from the Taylor cone (see Eq. 4), thereby creating the difference between the two cases. Obviously the effects of a changing standoff height would be less visible for small deviations, while errors due to large changes can be compensated further by offline methods such as iterative learning control (ILC) [11].

CONCLUSIONS

In this paper, we presented a novel vision sensing based approach for controlling droplet diameters in e-jet printing. While the improvements in closed loop performance are limited due to lack of dynamic process information, along with low temporal and spatial resolution, experimental evidence shows visual feedback as a valid method for increasing e-jet manufacturing precision.

Future work will investigate the use of ILC for compensation of repetitive errors and the implementation of sensors with increased resolution and improved signal to noise ratio.

ACKNOWLEDGMENT

The authors would like to thank Bokai Chen and Yi-Kai Wang for their initial work on image processing and data collection.

This work is supported by the NSF grant CMMI-1334204.

REFERENCES

[1] Park, J.-U., Hardy, M., Kang, S., Barton, K., Adair, K., Mukhopadhyay, D., Lee, C., Strano, M., Alleyne, A., Georgiadis, J., Ferreira, P., and Rogers, J., 2007. "High-resolution electrohydrodynamic jet printing". *Nature Materials,* ***6***(10), pp. 782–789.

[2] Youn, D.-H., Kim, S.-H., Yang, Y.-S., Lim, S.-C., Kim, S.-J., Ahn, S.-H., Sim, H.-S., Ryu, S.-M., Shin, D.-W., and Yoo, J.-B., 2009. "Electrohydrodynamic micropatterning of silver ink using near-field electrohydrodynamic jet printing with tilted-outlet nozzle". *Applied Physics A,* ***96***(4), pp. 933–938.

[3] Wang, K., Paine, M. D., and Stark, J. P. W., 2009. "Fully voltage-controlled electrohydrodynamic jet printing of conductive silver tracks with a sub-100m linewidth". *Journal of Applied Physics,* ***106***(2), pp. –.

[4] Poellmann, M. J., Barton, K. L., Mishra, S., and Johnson, A. J. W., 2011. "Patterned hydrogel substrates for cell culture with electrohydrodynamic jet printing". *Macromolecular Bioscience,* ***11***(9), pp. 1164–1168.

[5] Jayasinghe, S., Qureshi, A., and Eagles, P., 2006. "Electrohydrodynamic jet processing: An advanced electric-field-driven jetting phenomenon for processing living cells". *Small,* ***2***(2), pp. 216–219.

[6] Park, J.-U., Lee, J. H., Paik, U., Lu, Y., and Rogers, J. A., 2008. "Nanoscale patterns of oligonucleotides formed by electrohydrodynamic jet printing with applications in biosensing and nanomaterials assembly". *Nano Letters,* ***8***(12), pp. 4210–4216.

[7] Barton, K., Mishra, S., Alleyne, A., Ferreira, P., and Rogers, J., 2011. "Control of high-resolution electrohydrodynamic jet printing". *Control Engineering Practice,* ***19***(11), pp. 1266 – 1273.

[8] Mishra, S., Barton, K. L., Alleyne, A. G., Ferreira, P. M., and Rogers, J. A., 2010. "High-speed and drop-on-demand printing with a pulsed electrohydrodynamic jet". *Journal of Micromechanics and Microengineering,* ***20***(9).

[9] Choi, H. K., Park, J.-U., Park, O. O., Ferreira, P. M., Georgiadis, J. G., and Rogers, J. A., 2008. "Scaling laws for jet pulsations associated with high-resolution electrohydrodynamic printing". *Applied Physics Letters,* ***92***(12).

[10] Otsu, N., 1976. "A threshold selection method from gray-level histograms". *IEEE Transactions on Systems, Man and Cybernetics,* ***9***(1), pp. 62 – 66.

[11] Bristow, D., Tharayil, M., and Alleyne, A., 2006. "A survey of iterative learning control". *Control Systems, IEEE,* ***26***(3), pp. 96–114.